

Paper No. 18

AIRFLOW OVER HELICOPTER BLADES

by Michel Lecarme, Ingénieur de Recherche
Aérospatiale Division Hélicoptères, Marignane

1. SUMMARY

The subject of this lecture will be the study of airflow over helicopter blades, based on our observations made on a rotor having a diameter of 4.150 metres which was tested in the large wind tunnel at Modane.

We have made use of several operating processes to determine the nature of airflow over blades : smoke emission, pressure transducers, Mac Croskey's hot films, photographs of parietal tufts ; this lecture concerns mainly the last operating process, its analysis being facilitated by comparing actual positions, as shown on photos, and positions estimated according to the theory of L.R. Lucassen and H.J.G.C. Vodegel (NLR).

2. SYMBOLS

R	rotor radius	ρ	mass density of air
\bar{R} or x	relative radial distance	ρ_t	mass density of tuft
S	rotor area	dt	tuft diameter
σ	rotor solidity	f	coefficient of local speed
U	peripheral speed	Cn	coeff. of force normal to the tuft
V	airspeed	λ	tuft parameter
Λ or μ	advance ratio = V/U	pas g	collective pitch angle
ψ	azimuth angle	pas c or cp	cyclic pitch angle
M	advancing tip Mach number	X/C	relative chordwise location
Aq	shaft angle	Z	rotor lift, normal to the wind
A1	longitudinal tilt	\bar{Z}	rotor lift coefficient
			$= 100Z/\frac{1}{2} \rho S \sigma U^2 = 200 CLR/\sigma$

3. INTRODUCTION

The phenomena encountered during a rotor experimental study are numerous and complicated. Before dealing with airflow visualizations, it would be useful to recall some features of the experimental device and the rotor behaviour.

Figure 1 is an outside view of large Wind Tunnel S1 at Modane ; figure 2 shows the 8 metre diameter test section, the rotor and its stand, and the power plant ; the six-component balance and the 110 track slip ring are located under the hub, inside the shrouded pyramid ; the rotor is fully articulated ; the collective pitch control and the longitudinal cyclic pitch control are electro-hydraulic. The stroboscopic device used to photograph tufts is not visible, it is located above a port hole in the test section upper part.

4. TIP VORTICES

Interactions between blades and tip vortices are frequent phenomena. Figure 3 was published in nineteen seventy at the ICAS Congress in Roma ; it is the flash visualization of a filament of smoke winding round the tip vortex originated by the retreating blade, and the following blade hits this vortex, thus resulting in local disturbances that we were able to show up in many ways, especially by means of miniature pressure transducers. Interactions are important only for configurations in which the tip path plane is close to the horizontal.

We have plotted on the visualization boards, some curves which are the loci of the points where vortex interactions are possible. Figure 4 shows how these curves have been drawn.

For a three-bladed rotor, we have three types of interactions :

- a blade runs into the vortex generated by the preceding blade (curves 1)
- a blade runs into the vortex generated by the following blade (curve 2)
- a blade runs into its own tip vortex (curve 3)

5. VIBRATIONS AND LOADS

Often, it happens that a stall is shown up by visualization, but without divergency of rotor dynamic behaviour ; some comments are useful.

The most unpleasant consequence of stalling is the blade torsional vibration generated by the centre of pressure moving towards the trailing edge ; before this vibration becomes harmful, another condition is necessary, that is Kinetic pressure must be sufficient ; figure 5 shows chordwise Kinetic pressure curves versus Kinetic pressure at the tip of advancing blade ; this curves are called in France "Pascal's snails". When advance ratio increases, low Kinetic pressure area increases ; stalling may pass unnoticed with respect to dynamic behaviour.

Stalling development depends on control law ; we have five parameters to define a measuring configuration : rpm, airspeed, shaft angle, collective pitch, longitudinal cyclic pitch ; we may have a free longitudinal tilt (without cyclic pitch), or cancel this tilt by a high cyclic pitch, or choose a medium law. When Lock's number is low (it was our case) free tilt products a large upstream - downstream dissymetry of aerodynamic loads ; upstream area is overloaded and is stalling first ; figure 6 shows a map of loads measured using differential pressure transducers ; on the left : local average chordwise pressure, on the right : local CN ; longitudinal tilt value was high : 10.6 degrees, cyclic pitch was zero. A simple calculation shows that the first harmonic cosine term of aerodynamic moment about the flapping axis is proportional to the product of longitudinal tilt angle by blade density ; our measurements confirm calculated values. The most satisfactory dynamic behaviour is obtained by a medium control law ; performance characteristics are almost the same in the three cases.

6. THEORY OF TUFTLINES

The theory of tuft position on a helicopter blade was published in Luchvaarttechniek 2 (24/10/1969) by L.R. Lucassen and H.G.C. Vodegel, NLR. The first equation is very simple and is shown in Figure 7, together with an example of curves in rectangular coordinates ; this theory is not applicable inside the reverse flow circle, which is a sinusoid in this case. There is a small area where we find a duality of solutions, about an azimuth angle of 230 degrees ; the negative solutions are probably unsteady. For a physical point of view, this zone is critical because, if we follow a thread in the vicinity of $x = 0.4$, we see that it would rotate so quickly in this area its actual position becomes uncertain ; this fast rotation also exists for the local airspeed, so that the boundary layer is strongly sheared. Nevertheless, this fact is not very important because the critical zone includes very low kinetic pressures.

Figure 8 shows a more comprehensible aspect of the results derived from the theory, but with a complex mathematical expression ; these curves called "Tuftlines" are tangent in all points to the direction of tufts, in the absence of disturbance. Such curves are dependent on advance ratio and characteristics of tufts, grouped in the dimensionless coefficient λ .

When advance ratio increases, tufts are almost totally centrifugated at the end of retreating blade area ; we must anticipate some difficulty of interpretation as there may be airflow separations which will pass unnoticed ; a strong energy would be needed in the boundary layer to shake or divert a thread inside a field of high centrifugal acceleration and low kinetic pressure.

7. VISUALIZATIONS

Visualization device is applicable only at small incidence angles of tip path plane. There are :

- a stroboscopic flash installation fitted to a swivelling turret, where triggering of flashes is monitored by the rotor timing device supplying 128 electric pulses per revolution, one of which having a larger amplitude to define zero azimuth angle ;
- a television installation, remotely controlled and completed by a magnetoscope ;
- a photographic installation fitted to the swivelling turret ;
- a programmable electromechanical device for automatic operation of the camera, flashes and turret.

The programme used is the following : 32 photos per configuration, at 32 angles of azimuth, each photo including five exposures on five consecutive revolutions at the same azimuth (to show stability of tuft position).

Ranging, positioning of photos, and analysis of results take a long time. Figures 9 and 10 are two examples of our 40 maps of visualizations ; reduction ratio is $1/3.5$; the general view is distorted by perspective.

On figure 9, we have a low advance ratio and a high rotor lift, without cyclic pitch. The first vortex interaction line is shown, in red on the original map ; in this case, stall and torsional vibrations are beginning ; the interaction line is disturbed and initiates stall which appears here by a reverse flow towards the leading edge ; in the non disturbed areas, airflow is very stable.

The direction of threads in the second row is often different from that of the first row threads, because the overspeed coefficient included in parameter λ is not constant along the chord ; the recommended values in the theory are well adapted to the first row located at 25 % of chord ($C_n \sim 2$, $f \sim 1.1$). At the blade tip, it happens often that threads are less centrifugated than theoretically explained ; in our opinion, the threads are affected by the birth of tip vortex.

On figure 10 (Map 37), we have a high advance ratio and longitudinal tilt is cancelled entirely by cyclic pitch ; stall is significant in spite of a moderate value of rotor lift ; the upstream overloads of free tilt tests have disappeared, but stall, in zero tilt tests, is premature and strong.

The tuft method is not applicable to the study of shock-waves and very brief vortex interactions in the first quadrant, because of tuft inertia.

8. INTERPRETATIONS

During our tests, an interesting help was brought by Mac Croskey's hot films. One blade only was fitted with tufts, the other blades being fitted with a dozen of hot films ; each active filament was running parallel to the leading edge ; temperature of these filaments is kept constant by using an appropriate electronic device, and electrical variations characterize thermal transfers within the boundary layer.

An example of signals from hot films is shown on figure 11, for two chordwise positions on upper surface, with an advance ratio of 0.50 ; collective pitch increases from top to bottom. Signals from hot films vary between two sinusoids, one being laminar and the other turbulent ; in the case of figure 11 we are always in turbulent conditions ; when stall appears, signal fluctuations increase.

In order to characterize nature of airflow, we have drawn the zones where tuft directions do not conform to the theory, zones called "non tuftlines areas" in figures 12, 13 and 14. The "inside" zone is undercentrifugated, the "outside" zone is overcentrifugated ; in the "big stall" zone, the tufts have no average direction or are directed towards the leading edge, and stall is obvious. According to the signals from hot films, overcentrifugated zones are generally stalled ; when increasing of collective pitch gives a stall beginning, overcentrifugated zones are wider than disturbed zones of hot films ; beyond, stalled zones are the same.

Figure 12 shows the development of stall when collective pitch is increasing, for a very small advance ratio. We can clearly see that stall is developing up-stream along the first interaction line (without cyclic pitch) ; vibration troubles were occurring about Z 17 ; on the last case Z 21.1, there is a small normal airflow area at an azimuth angle of 270 degrees ; such an area is not exceptional.

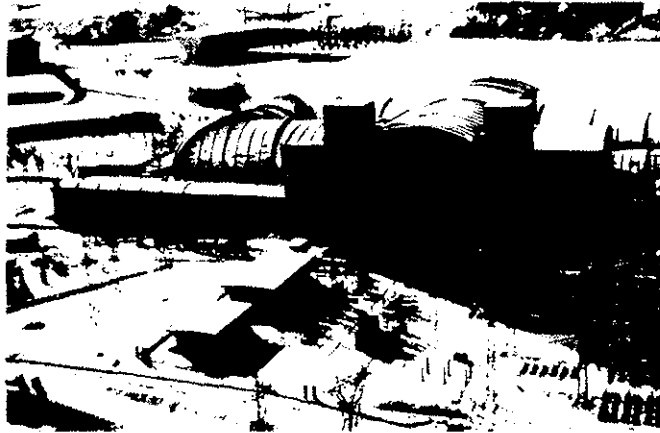
Figures 13 and 14 show the influence of cyclic pitch on the stall for a large advance ratio : 0.50. High values of oblique attack angles and low values of kinetic pressures on the retreating blade indicate that the phenomena are complex and difficult to interpret. As for the configuration of figure 13, vibration troubles occurred immediately after the second case (Z 14.15) ; vortex interaction do not affect stall ; other previous tests have shown that chordwise pressure distributions were disturbed by vortices in the transonic zone of the first quadrant.

Even by cancelling the longitudinal tilt through the cyclic pitch, we did not succeed in reaching high lift values (for the advance ratio of 0.50) ; the cyclic pitch angle of the fifth case was ten degrees and we could not go beyond that value. The vibration divergence occurred between the third and fourth case, for a very moderate lift value. Reverse flow circles are blank, because the tuftlines theory is not applicable in this zone.

We have made several visualizations at advance ratios higher than 0.60, at a tip Mach number of about 0.90 ; such tests are difficult to run, and results are often confusing because there is a divergence between indications from tufts and hot films.

9. CONCLUSION

Visualization by photographs of tufts is a very good operating process for understanding airflow over helicopter blades, especially the development of stall ; fitting of blades is simple and tests are quickly run ; nevertheless the experimental device is expensive and study of results requires a long time ; the tuftlines theory is an interesting help in this study. Validity of visualization method now ranges from hovering to an advance ratio of 0.60.



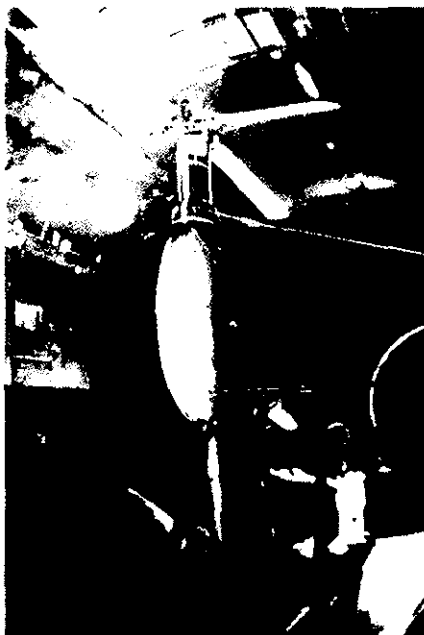
WIND TUNNEL S 1

Figure 1



VORTEX INTERACTION

Figure 3



TEST SECTION

Figure 2

BLADES-TIP VORTICES INTERSECTIONS $A=0.30$

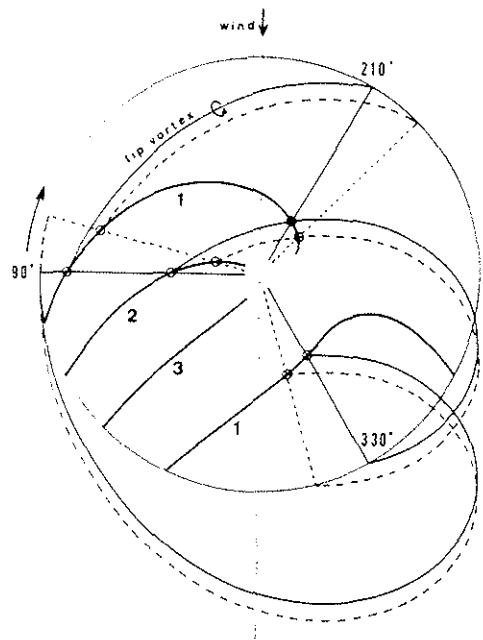


Figure 4

CHORDWISE KINETIC PRESSURES

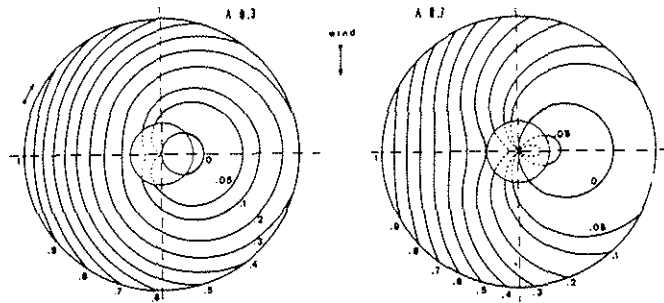
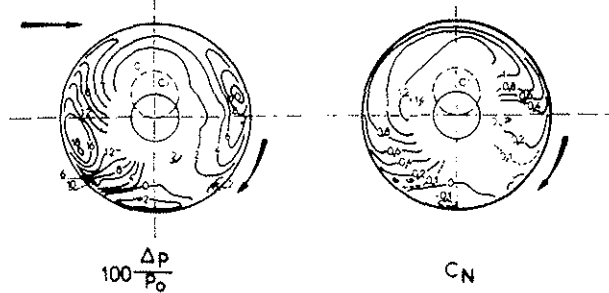


Figure 5

$V/\Omega R = 0,50$

$\alpha_D = -5,4 \text{ degrés}$ $\theta = 12,5 \text{ degrés}$

$10^3 C_{LR}/\sigma = 64,5$ $10^3 C_{XR}/\sigma = 3,67$ $10^3 C_p/\sigma = 6,33$



LOCAL LOADS

Figure 6

LINES FOR CONSTANT TWT ANGLE

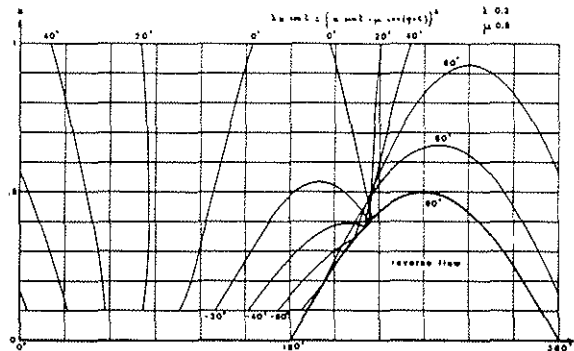


Figure 7

Positione théorique des fils (Tuffinas)

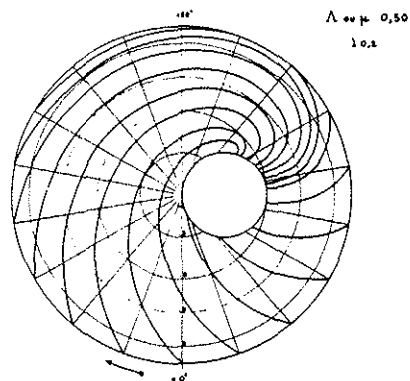
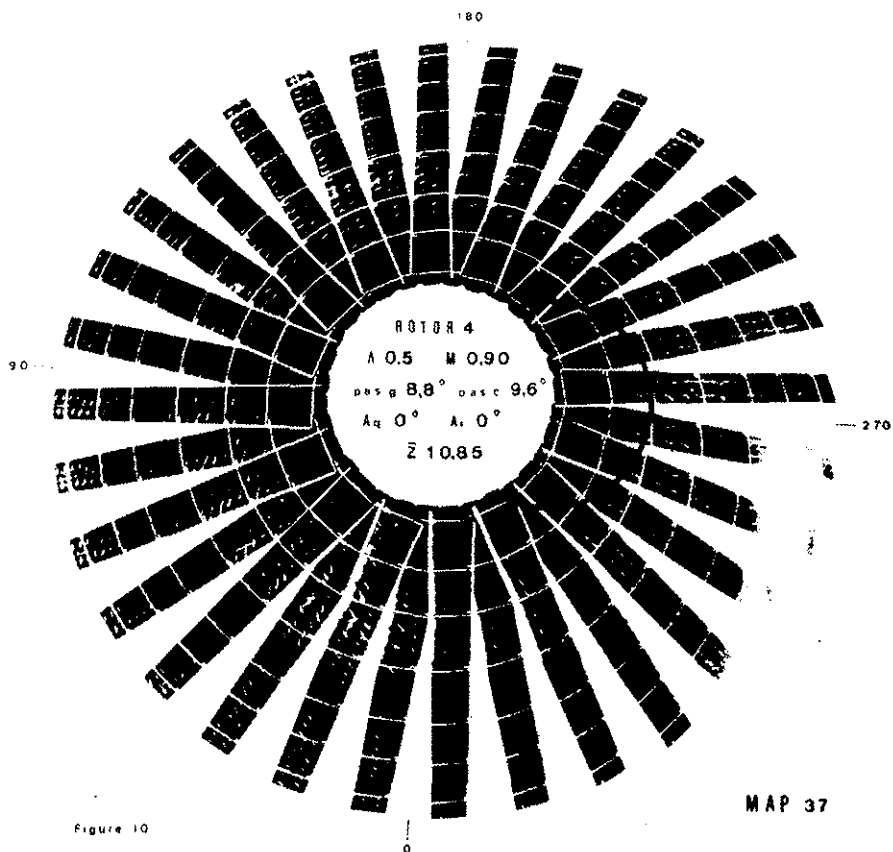
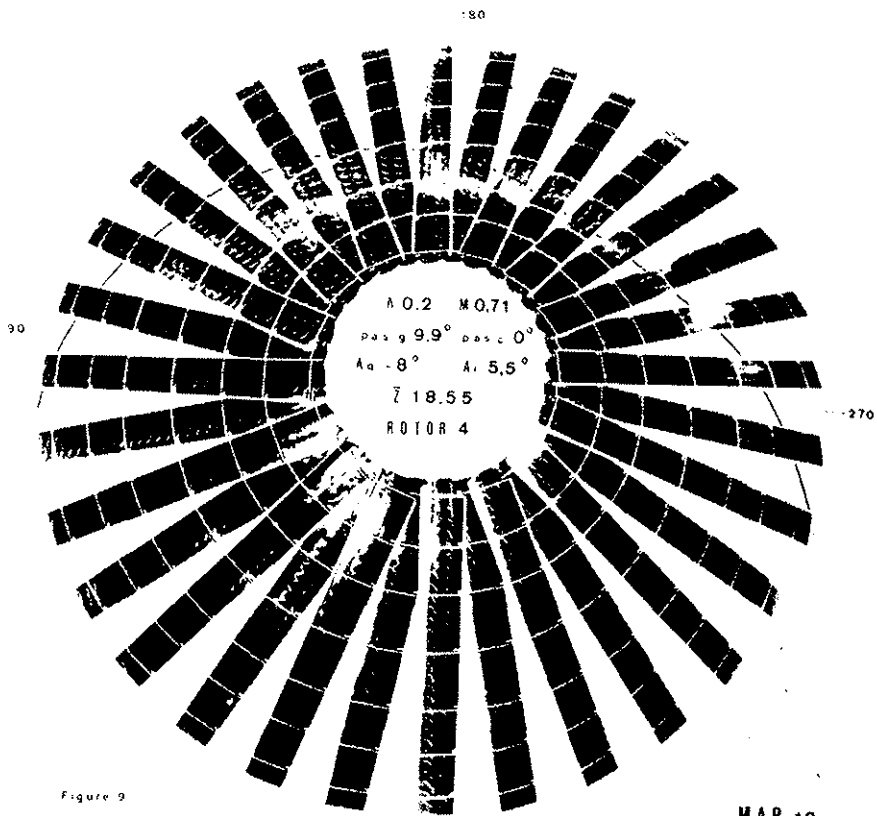
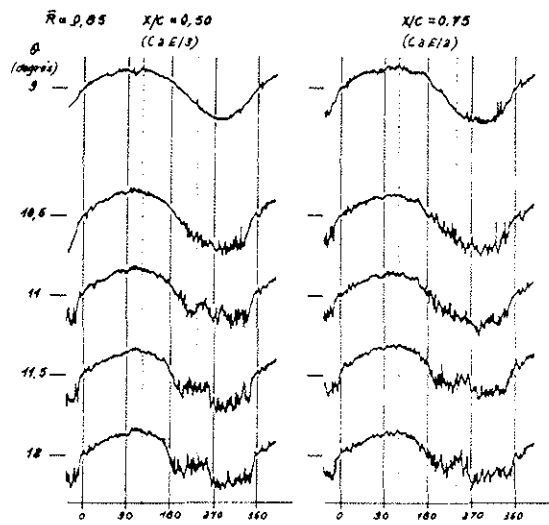


Figure 8





SIGNALS FROM HOT FILMS

Figure 11

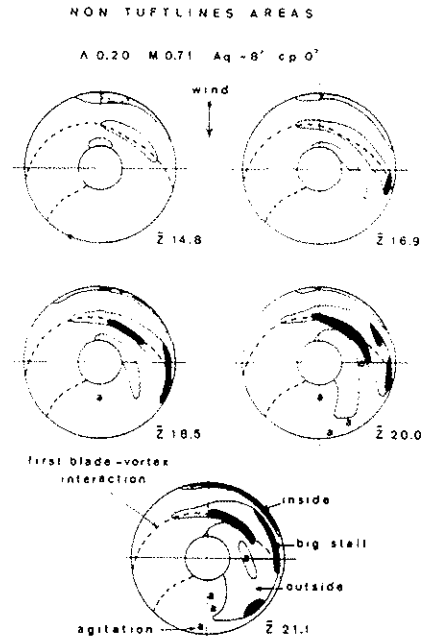


Figure 12

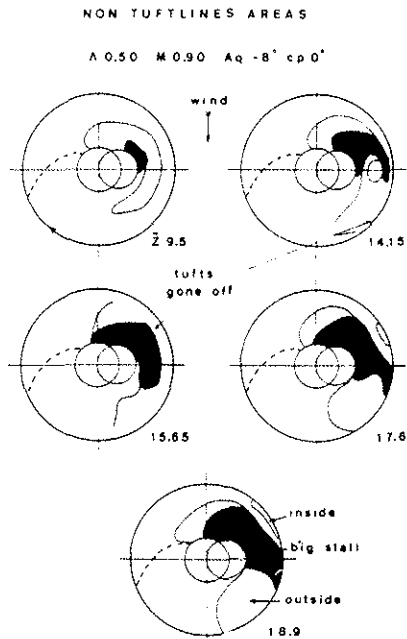


Figure 13

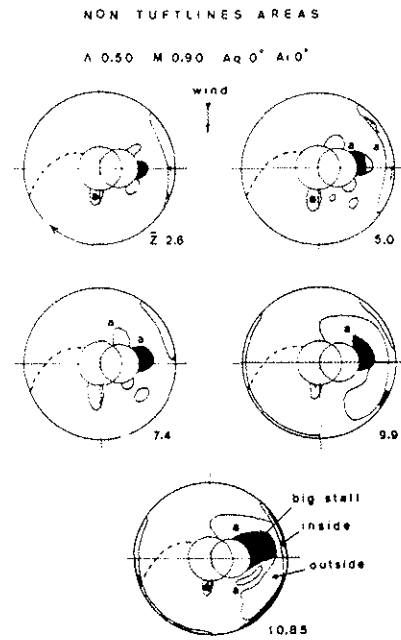


Figure 14